Differential Effects of Base Excision Repair Factor Depletion on Cellular Sensitivity to PARG Inhibition in Ovarian Cancer Cells

By

Zhiying He

BS, University of California, Davis, 2024

Thesis

Submitted in partial fulfillment of the requirements for the Degree of Master of Science in the Graduate Program of Biotechnology at Brown University

PROVIDENCE, RHODE ISLAND

April 01, 2026

This thesis by (Zhiying He) is accepted in its present form by the Graduate Program in Biotechnology as satisfying the thesis requirements for the degree of Master of Science

Date 4/30/2026 Signature: DocuSigned by: Robert W. Sobol 480651B20F9E4F7...

Robert W. Sobol, PhD; Advisor

Date 5/2/2026 Signature: DocuSigned by: EDITH MATHIOWITZ E063C09A6AB6428...

Dr. Edith Mathiowitz, Reader

Date 4/30/2026 Signature: Signed by: E K 310C8FF090B5412...

Dr. Eric Huang, Reader

Approved by the Graduate Council

Date _____ Signature: _____

David P. Lindstrom, Dean of the Graduate School

Acknowledgments

I would like to express my sincere gratitude to Dr. Robert W. Sobol for his exceptional support and guidance throughout my master's program and for guiding me into the realm of laboratory research.

I am grateful to all members of the Sobol Lab for their support, collaboration, and for creating a welcoming and stimulating research environment.

I also thank my friends for their constant support, understanding, and encouragement throughout my long academic journey.

I would like to thank my cat for providing comfort and companionship during both challenging and joyful times.

Finally, I would like to extend my deepest appreciation to my family, especially my parents, for their unwavering support and encouragement in my academic journey. Their belief in me has made this achievement possible.

Abstract

Base excision repair (BER) is a critical DNA repair pathway that resolves base and single-strand DNA damage to help maintain genomic stability. Key BER proteins [*e.g.,* XRCC1, DNA polymerase β (POLB), DNA ligase III (LIG3), and aprataxin (APTX)] operate in a coordinated manner, along with poly(ADP-ribose) polymerases 1 and 2, to facilitate efficient repair. In multiple studies, disruption of poly(ADP-ribose) (PAR) metabolism, by inhibiting poly(ADP-ribose) glycohydrolase (PARG), has been demonstrated to impair DNA repair and induce replication stress. However, the contribution of individual BER components to the cellular response to PARG inhibition remains poorly defined in the literature. In this study, we have evaluated the roles of selected BER factors in modulating cellular sensitivity to PARG inhibition in ovarian cancer cells. More specifically, ES-2 cells were subjected to siRNA-mediated knockdown of XRCC1, POLB, LIG3, and APTX, and protein depletion was confirmed by immunoblotting. Cell viability was evaluated following treatment with the PARG inhibitor PDD00017272. Depletion of XRCC1 was correlated with a consistent increase in sensitivity to PARG inhibition across biological replicates. LIG3 knockdown also reduced cell viability in response to PARG inhibition, though the magnitude of this effect varied. In contrast, POLB depletion produced modest, less consistent changes, whereas APTX knockdown had minimal impact on the cellular response under the conditions tested. Overall, these results suggest that BER proteins play distinct roles in how cells respond to PARG inhibition. XRCC1, in particular, stands out as a key factor in maintaining cell viability under these conditions. While these findings are compelling, the variability within certain experimental groups and our limited number of biological replicates suggests that these results should be viewed as preliminary. Therefore, in future studies, it will be essential to use a broader range of experimental models to pin down the exact mechanisms at play.

Introduction

DNA damage is a continuous and inevitable process in human cells. It stems from endogenous metabolic activities, such as reactive oxygen species, and exogenous environmental factors, including radiation and chemotherapeutic agents. Unrepaired DNA lesions accumulate over time, driving genomic instability, which is a fundamental hallmark of cancer initiation and progression. To safeguard genomic integrity, cells utilize a sophisticated network of DNA repair pathways that detect, signal, and repair DNA damage in a coordinated fashion [1,2]. Key mechanisms such as base excision repair (BER), nucleotide excision repair (NER), homologous recombination (HR), and non-homologous end joining (NHEJ) work collectively to preserve cellular homeostasis and DNA integrity [3,4].

Among these pathways, BER primarily repairs base and single-strand DNA damage, such as oxidized bases, abasic sites, and single-strand breaks. BER is a finely tuned process comprising several steps. It involves lesion recognition, end processing, gap filling, and ligation. Key proteins, including XRCC1, POLB, LIG3, and APTX, mediate this process. XRCC1 serves as a versatile scaffold protein that facilitates multiple enzymatic steps, including gap filling by DNA polymerase β and nick sealing by DNA ligase III. The interaction between XRCC1 and POLB is vital for efficient recruitment and stabilization of the repair machinery. Following nucleotide insertion, LIG3 catalyzes the final ligation step, whereas abortive ligation events generate adenylated DNA intermediates that are resolved by Aprataxin (APTX). When this delicate balance is disrupted, repair intermediates accumulate, triggering significant cellular stress [5,6].

In response to DNA damage, activation of poly(ADP-ribose) polymerases (PARP1 and PARP2) leads to the synthesis of poly(ADP-ribose) (PAR), which operates as a signaling platform for recruiting DNA repair proteins to damage sites [7,9]. PARylation promotes assembly of repair

complexes, such as XRCC1, POLB, APTX, and LIG3, facilitating efficient repair of single-strand breaks [5,8]. Following repair completion, PAR is degraded by poly(ADP-ribose) glycohydrolase (PARG), enabling release of BER proteins and restoration of chromatin structure [9,10].

PARP inhibitors (PARPi) have already achieved notable clinical success in treating tumors with homologous recombination deficiency (HRD), particularly those with BRCA1/2 mutations [11]. At the same time, PARG inhibitors (PARGi) have emerged as a promising therapeutic strategy by disrupting PAR homeostasis and inducing replication stress [12–14]. Mechanistically, inhibition of PARG prevents PAR degradation, thereby blocking the release of BER proteins from DNA damage sites and impairing repair completion [12,13]. As a result, persistent PAR signaling leads to the accumulation of DNA repair intermediates and replication-associated DNA lesions. This sustained signaling promotes replication stress, characterized by the accumulation of single-stranded DNA gaps and activation of checkpoint pathways such as ATR/CHK1, ultimately contributing to cell death [13–15].

Individual BER proteins play distinct mechanistic roles within the repair pathway, suggesting that their disruption may differentially affect cellular responses to DNA damage and to therapeutic inhibition. XRCC1 serves as a primary scaffold coordinating recruitment and retention of essential BER factors. Within this framework, POLB and LIG3 handle the downstream gap-filling and ligation steps, while APTX serves as a specialized safeguard to resolve abortive repair intermediates. This fluid turnover of BER proteins is governed by PARP/PARG-dependent signaling, which creates a necessary balance between protein docking and release. While the functional interplay between the BER machinery and PAR dynamics is clear, the specific contributions of individual proteins to PARG inhibitor sensitivity are an open question.

Understanding which components are most critical to this vulnerability could reveal new therapeutic dependencies.

The present study addresses this issue by investigating the functional roles of key BER genes using siRNA-mediated knockdown in ovarian cancer cells. By targeting XRCC1, POLB, LIG3, and APTX, we evaluated how BER disruption influences cell viability and sensitivity to the PARG inhibitor PDD00017272. We hypothesize that impairment of BER enhances sensitivity to PARG inhibition and that distinct BER components modulate therapeutic response differentially. These findings offer mechanistic insights into BER-dependent DNA repair vulnerabilities and may inform the development of improved therapeutic strategies targeting DNA repair pathways in ovarian cancer.

Materials and Methods

Materials

All reagents, including antibodies, inhibitors, cell line, and software used in this study, are listed in **Table S1**, along with their catalog numbers and sources.

Small interfering RNAs (siRNAs) targeting BER genes, such as XRCC1 (Horizon, Cat# M-009394-01-0005), POLB (Horizon, Cat# M-005164-01-0005), LIG3 (Horizon, Cat# M-009227-02-0005), and APTX (Horizon, Cat# M-013368-02-0005), as well as a non-targeting control siRNA(Horizon, Cat# D-001206-13-05), have been utilized for siRNA transfection.

The PARG inhibitor PDD00017272 (Tocris, Cat# 7006) was used for drug treatment experiments and dissolved in dimethyl sulfoxide (DMSO) (Thermo Fisher Scientific, Cat# 3176) to prepare a 10 mM stock solution.

Cells and cell culture

The ES-2 human ovarian cancer cell line (ATCC, Cat# CRL-1978) was cultured in RPMI 1640 medium (Corning, Cat# 10-040-CV) containing 10% heat-inactivated fetal bovine serum (FBS) (Atlanta Biologics, Cat# S11150), L-glutamine (Gibco, Cat# 25030-081), and 1% penicillin-streptomycin (100 U/mL and 100 µg/mL) (Thermo Fisher Scientific, Cat# 15140-122). Cells were maintained in a humidified incubator at 37°C/5% CO_2 and passaged regularly to maintain exponential growth.

RNAiMAX Transfection

ES-2 cells were seeded in 60 mm culture dishes at approximately 2×10^5 cells per dish and cultured overnight until reaching 60–70% confluence before transfection. For siRNA transfection, siRNA and Lipofectamine RNAiMAX (Thermo Fisher Scientific, Cat# 13778075) were diluted separately in Opti-MEM reduced serum medium (Thermo Fisher Scientific, Cat# 31985062). For each transfection, 150 µL Opti-MEM containing 3 µL siRNA (10 µM stock) was prepared. Furthermore, 150 µL Opti-MEM containing 9 µL Lipofectamine RNAiMAX was prepared in separate tubes. Subsequently, diluted siRNA and Lipofectamine RNAiMAX solutions were combined and gently mixed, followed by incubation at room temperature for 5 minutes to allow formation of siRNA–lipid complexes.

Meanwhile, the culture medium was replaced with fresh complete growth medium supplemented with FBS. The siRNA–lipid complexes prepared in serum-free Opti-MEM were added dropwise to the cells, and plates were gently rocked to ensure even distribution. Cells were incubated at 37°C / 5% CO_2 for 24 hours following transfection. Next, the culture medium was replaced with fresh complete growth medium, and cells were further incubated for an additional 48 hours to allow sufficient gene knockdown before downstream analysis, including cell lysate preparation and immunoblotting.

Cell protein lysate preparation

Following siRNA transfection, cells were harvested for protein analysis, as follows. Cells were seeded in a 100 mm culture dish at approximately 4×10^5 cells per dish and cultured until reaching 70–80% confluence. At 72 hours post-transfection (24 hours followed by media replacement and an additional 48 hours), the culture medium was completely removed, and cells were washed twice

with cold phosphate-buffered saline (PBS) (Corning, Cat# 21-031-CV). After complete removal of PBS, an appropriate volume of 4× Laemmli sample buffer (Bio-Rad, Cat# 1610747) supplemented with β-mercaptoethanol (Aldrich, Cat# SHBH7147) at a final concentration of 50 µL per 1 mL of sample buffer was added directly to the cells. Cells were then scraped with a cell scraper, and the lysate was transferred to 1.5-mL microcentrifuge tubes. Samples were heated at 98°C for 5 minutes to denature proteins, and the protein concentration was determined using a NanoDrop 2000c Spectrophotometer.

Immunoblot

Equal amounts of protein (30 µg) were loaded onto 4–12% Bis-Tris polyacrylamide gels (Invitrogen, Cat# NP0323BOX) and separated by SDS-PAGE at 100–120 V for approximately 1.5 to 2 hours. Protein molecular weight markers (Smobio, Cat# PM2610) were used as size standards. Following electrophoresis, proteins were transferred onto nitrocellulose membranes (Bio-Rad, Cat# 1704270) for 18 min using a Trans-Blot Turbo transfer system (Bio-Rad). Membranes were blocked in 5% non-fat milk prepared in Tris-buffered saline containing 0.1% Tween-20 (TBST) for 1 hour at room temperature. Membranes were incubated with primary antibodies against XRCC1(Abcam, Cat# ab134056), DNA polymerase β (POLB) (Abcam, Cat# ab26343 or ab175197), DNA ligase III (LIG3) (Abcam, Cat# ab223739), and aprataxin (APTX) (Abcam, Cat# ab192598) overnight at 4°C. After primary antibody incubation, membranes were washed three times with TBST for 10 minutes each. Then, membranes were incubated with Goat Anti-Rabbit IgG (H + L)-HRP Conjugate secondary antibody (Bio-Rad, Cat# 170-6515) for two hours at room temperature, followed by three additional washes with TBST. Protein bands were detected with an

enhanced chemiluminescence (ECL) substrate and visualized on a ChemiDoc imaging system. Histone H3(Cell Signaling Technology, Cat# 4499) was used as a loading control for normalization.

Cell viability assay

Cell viability following PARG inhibitor treatment was determined using an imaging-based assay. For viability experiments, cells were seeded into 96-well plates at an appropriate density of 800 cells/well and incubated for 24 hours. Next, cells were treated with a range of concentrations of the PARG inhibitor PDD00017272 using serial dilutions, as depicted in the figures. Drug treatment was performed without removing the conditioned medium. After 5 days (120 hours) of drug treatment, cells were stained with Hoechst 33342 (Thermo Fisher Scientific, Cat# 62249) to label total nuclei and propidium iodide (PI) (Sigma-Aldrich, Cat# P4170) to specify dead cells. Staining was performed for 15 minutes at 37°C. Total and dead cells were quantified using a Celigo S imaging cytometer (Nexcelom Bioscience) by capturing Hoechst fluorescence (excitation/emission: 377 nm/470 nm) and PI fluorescence (excitation/emission: 531 nm/629 nm). Cell viability was computed based on the ratio of live to total cells, and dose-response curves were generated to evaluate sensitivity to PARG inhibition under diverse siRNA knockdown conditions.

Results

Efficient knockdown of BER factors XRCC1, POLB, LIG3, and APTX

To investigate the role of BER factors in the cellular response to PARG inhibition, we first established siRNA-mediated knockdown of key BER proteins, including XRCC1, POLB, LIG3, and APTX. Immunoblot analysis confirmed the efficient depletion of each target protein following siRNA transfection compared to non-targeting control (siNON) cells. Specifically, XRCC1 knockdown was validated across three independent biological replicates, demonstrating a consistent and robust reduction in XRCC1 protein levels (**Figure 1A-C**). Likewise, POLB protein levels were markedly reduced upon siPOLB transfection across all three independent replicates, further confirming the efficacy of the silencing approach (**Figure 1D–F**). In parallel, knockdown of LIG3 and APTX was confirmed by immunoblotting. LIG3 protein levels were clearly reduced in siLIG3-treated cells across three independent replicates (**Figure 2A–C**), while APTX depletion was consistently observed in siAPTX-treated cells (**Figure 2D–F**). In all experiments, histone H3 was utilized as a loading control. Overall, these outcomes confirm robust and reproducible depletion of BER factors, enabling downstream functional analyses.

Loss of XRCC1 enhances cellular sensitivity to PARG inhibition

Given the established role of BER proteins in resolving DNA repair intermediates, we next evaluated whether their depletion alters cellular sensitivity to PARG inhibition. Cell viability assays were performed following exposure to increasing concentrations of PARGi for 120 hours. In control siNON cells, PARG inhibition resulted in relatively modest effects on cell viability. In contrast, XRCC1 knockdown resulted in a pronounced reduction in cell viability upon PARGi

treatment across three independent biological replicates (**Figure 3A–C**). This enhanced sensitivity suggests that loss of XRCC1 compromises the cell's tolerance to PARG inhibition, consistent with a potential functional interaction between BER deficiency and PARG inhibition.

POLB depletion shows variable effects on PARG inhibitor response

Next, we evaluated the impact of POLB knockdown on PARG inhibitor sensitivity. Compared to XRCC1 depletion, POLB knockdown led to more modest and variable effects on cell viability following PARGi treatment (**Figure 3D–F**). While some reduction in viability was observed at higher concentrations of PARGi, the magnitude of sensitization was less consistent across replicates. These results demonstrate that although POLB contributes to BER, its loss may have a less pronounced or context-dependent effect on PARGi sensitivity compared to XRCC1.

LIG3 knockdown increases sensitivity to PARG inhibition

To further analyze the contribution of BER components to the cellular response to PARG inhibition, we examined the impact of LIG3 depletion on cell viability. Following exposure to increasing concentrations of a PARG inhibitor for 120 hours, LIG3 knockdown cells exhibited reduced cell viability compared to siNON controls across independent biological replicates (**Figure 4A–C**). This suggests that LIG3 depletion may enhance cellular sensitivity to PARG inhibition. Notably, the magnitude of this sensitization exceeded expectations, surpassing what might be predicted from the established role of LIG3 in the BER pathway or from previous literature. While this suggests a potentially context-dependent requirement for LIG3 in the cellular response to PARG inhibition, we must also consider the influence of experimental variables. Factors such as

fluctuating knockdown efficiency or subtle shifts in culture conditions across replicates could contribute to this pronounced phenotype. Further investigation is required to determine whether this reflects a unique biological dependency or inherent experimental variability.

APTX depletion has minimal or variable impact on PARG inhibitor sensitivity

Finally, we investigated the effect of APTX knockdown on the response to PARG inhibitors. In contrast to XRCC1 and LIG3 depletion, APTX knockdown did not result in a strong or consistent sensitization to PARG inhibition (**Figure 4D–F**). Cell viability in siAPTX-treated cells remained comparable to that of control cells across most PARGi concentrations, with only minor or variable differences observed between replicates.

Overall summary

Collectively, these results demonstrate that depletion of specific BER factors differentially affects cellular sensitivity to PARG inhibition. In particular, loss of XRCC1 and LIG3 markedly enhances PARGi-induced cytotoxicity, whereas depletion of POLB and APTX exhibits more modest or variable effects. These findings support a model in which BER components play distinct roles in maintaining cell viability under PARG inhibition and suggest that disrupting key BER factors, particularly XRCC1 and LIG3, may sensitize cells to PARG-targeted therapies.

Discussion

The integrity of the BER pathway is essential for maintaining cellular tolerance to DNA damage. In this study, we investigated how depletion of key BER factors modulates cellular sensitivity to PARG inhibition in ovarian cancer cells. Our results demonstrate that the disruption of BER components affects PARG inhibitor response in different ways. XRCC1 depletion produced the most consistent sensitization, while LIG3 showed a pronounced but variable effect. In contrast, POLB and APTX exhibited comparatively modest or inconsistent phenotypes.

Recent studies have demonstrated a direct functional correlation between replication-associated BER/single-strand break repair (SSBR) and cellular responses to PARG inhibition [20,21]. Inhibition of PARG disrupts PAR turnover, leading to persistent PARylation, impaired disassembly of repair complexes, and accumulation of DNA repair intermediates. These defects are particularly detrimental during the S phase. At this stage, unresolved lesions can interfere with replication fork progression and trigger ATR/CHK1-mediated checkpoint signaling [13–15,20]. Furthermore, sensitivity to PARG inhibitors has been demonstrated to correlate with the accumulation of single-stranded DNA gaps, further underscoring the importance of replication-associated repair processes [15,19]. Within this framework, BER/SSBR capacity emerges as a key determinant of cellular tolerance to PARG inhibition.

Among the proteins tested, XRCC1 depletion resulted in the largest increase in sensitivity to PARG inhibition. This outcome aligns with its role as a central scaffold protein in BER, coordinating the recruitment and stabilization of multiple repair factors. Moreover, XRCC1 facilitates interactions among key enzymes, including POLB and LIG3, thereby ensuring efficient repair of single-strand DNA damage [5,24]. Loss of XRCC1 likely disrupts multiple steps of the repair process concurrently, leading to the accumulation of unrepaired single-strand breaks and repair

intermediates. Importantly, BER factors such as XRCC1 are actively recruited to DNA damage sites in replicating cells via a PAR-dependent mechanism. These factors play a critical role in resolving lesions that emerge during DNA replication [20]. In this context, unrepaired single-strand breaks are particularly deleterious, as they can interfere with replication fork progression or be converted into more cytotoxic DNA lesions upon replication fork encounter. Under conditions of PARG inhibition, where PAR turnover is impaired, the timely resolution of these replication-associated repair intermediates is further compromised. Persistent PARylation can delay the disassembly of repair complexes and exacerbate the accumulation of DNA lesions, thereby elevating replication stress and promoting activation of ATR/CHK1-mediated checkpoint signaling pathways [20,23]. These mechanisms align with previous studies showing that PARG inhibition induces replication-associated DNA damage. Specifically, this leads to an accumulation of single-stranded DNA (ssDNA) gaps, which correlate strongly with cells' sensitivity to these PARG inhibitors [19]. Overall, these findings suggest that XRCC1 plays a critical role in maintaining replication fork stability by facilitating the resolution of DNA repair intermediates during S phase. Loss of XRCC1 increases cellular vulnerability to PARG inhibition by allowing replication-associated DNA damage to accumulate, ultimately reducing cell viability.

In contrast, POLB depletion resulted in more modest and variable effects on sensitivity to PARG inhibition. While POLB plays a vital role in gap-filling during base excision repair, the relatively weak phenotype observed here differs from recent studies demonstrating that reduced POLB expression can enhance cytotoxicity in response to alkylating agents and to PARG inhibition [18]. In addition, POLB has been shown to impact replication checkpoint signaling through PAR-dependent mechanisms, further linking its function to replication-associated stress responses [19]. One possible explanation for this discrepancy is differences in the experimental systems. Prior

studies have largely examined conditions of sustained POLB deficiency or altered expression levels, whereas the present study employs siRNA-mediated knockdown, which may result in incomplete depletion of POLB protein. Residual POLB activity, together with compensatory polymerases such as DNA polymerase λ [16,17], may preserve sufficient repair capacity to buffer the effects of POLB loss. Furthermore, the impact of POLB on PARG inhibitor sensitivity may be highly context-dependent, particularly with respect to the extent of replication stress and the cellular capacity to activate checkpoint responses. Thus, while our findings confirm that POLB modulates the response to PARG inhibition, they suggest that partial depletion alone cannot fully replicate the sensitization observed in other systems. This underscores the importance of considering both the experimental context and the degree of protein loss when interpreting BER-dependent responses to PARG inhibition.

Similarly, APTX depletion had minimal impact on PARG inhibitor sensitivity. APTX is known to resolve abortive DNA ligation intermediates produced during base excision repair, thereby preventing the accumulation of adenylated DNA ends [5,6]. However, our findings suggest that this function may not be a major determinant of the cellular response to PARG inhibition under the conditions tested. One possible explanation is that abortive ligation intermediates are not the predominant source of DNA damage induced by PARG inhibition. Instead, PARG inhibition primarily triggers replication-associated stress, characterized by the accumulation of single-stranded DNA gaps and the subsequent activation of ATR-dependent checkpoint pathways [13–15, 20]. In this context, repair steps previously involved in BER, such as damage recognition and gap filling, may play a more critical role in maintaining genome stability than resolving abortive ligation intermediates. Additionally, alternative repair mechanisms may compensate for APTX loss,

further reducing its impact on cellular sensitivity. Overall, these considerations suggest that APTX plays a more context-dependent or secondary role in modulating response to PARG inhibition.

Notably, LIG3 knockdown led to greater sensitivity to PARG inhibition than expected. Although LIG3 is primarily involved in the final ligation step of BER, this result may reflect a broader role in maintaining genome stability, particularly under conditions of replication stress. LIG3 functions in complex with XRCC1 to complete the repair of single-strand breaks, and disruption of this step can result in the persistence of DNA strand break intermediates [5]. In the presence of PARG inhibitors, PAR turnover is hindered, and repair complexes remain aberrantly stabilized on DNA. These conditions suggest that inefficient ligation could significantly worsen the buildup of repair intermediates. These unresolved lesions are particularly problematic during DNA replication, where they may interfere with replication fork progression or lead to fork collapse, thereby increasing cellular sensitivity to PARG inhibition. This interpretation aligns with recent findings highlighting the importance of replication-associated BER/SSBR in determining PARG inhibitor response [20]. However, the magnitude of the observed sensitization, combined with inter-replicate variability, suggests that this result should be interpreted with caution. Variability in knockdown efficiency or experimental conditions may contribute to this phenotype. Therefore, additional studies will be required to determine whether this reflects a true biological dependency or experimental variability.

Importantly, it should be noted that the present study utilized siRNA-mediated knockdown rather than complete gene knockout. This distinction may contribute to the relatively modest phenotypes observed for certain targets, such as POLB and APTX. Unlike knockout models, knockdown approaches often result in partial protein depletion, potentially allowing residual repair activity to persist. This incomplete loss of function could mask the full contribution of these proteins to BER

and to the cellular response to PARG inhibition. Therefore, future studies using CRISPR/Cas9 to generate stable knockout systems will be essential for fully defining the specific roles of individual BER components.

In addition, variability observed across biological replicates represents another important limitation of this study. Differences in knockdown efficiency, cell culture conditions, or experimental handling may have contributed to the variability in response, particularly for targets with more subtle effects. Increasing the number of biological replicates and incorporating additional experimental controls will be imperative to enhance the robustness and reproducibility of these findings.

Overall, our results support a model in which BER disruption triggers the accumulation of DNA repair intermediates and increases replication stress. This cascade ultimately increases cellular dependence on PAR metabolism. Under conditions of PARG inhibition, impaired PAR turnover further exacerbates these defects, ultimately reducing cell viability. These findings are consistent with recent studies demonstrating that targeting PARG in combination with defects in DNA repair pathways can produce enhanced cytotoxic effects [21].

Future work should also explore the molecular mechanisms underlying the differential sensitivity observed among BER proteins, especially the unexpected effect of LIG3. Similarly, additional assays, such as analysis of DNA damage markers, replication stress indicators, and PAR accumulation, would provide deeper insight into how BER disruption modulates the cellular response to PARG inhibition. These outcomes may also serve as a basis for future studies exploring the potential relationship between BER protein expression and response to PARG-targeted therapies.

References

1. Hopkins, J.L., et al. (2022). DNA repair defects in cancer and therapeutic opportunities. *Cancers*, 14, 8973847.
2. Negrini, S., Gorgoulis, V.G. and Halazonetis, T.D. (2010) Genomic instability — hallmark of cancer. *Cell*, 144, 646-674.
3. Jackson, S.P. and Bartek, J. (2009). The DNA-damage response in human biology and disease. *Nature*, 461, 1071-1078.
4. Ciccia, A. and Elledge, S.J. (2010). The DNA damage response: making it safe to play with knives. *Mol Cell*, 40, 179-204.
5. Almeida, K.H. and Sobol, R.W. (2007) A unified view of base excision repair: lesion-dependent protein complexes regulated by post-translational modification. *DNA Repair (Amst)*, 6, 695-711.
6. Krokan, H.E. and Bjørås, M. (2013) Base excision repair. *Cold Spring Harb Perspect Biol*, 5, a012583.
7. Ahel, I., et al. (2008). Poly(ADP-ribose)-binding domains. *Nature*, 451, 81-85.
8. Koczor, C.A., et al. (2021). Temporal dynamics of base excision repair protein complex assembly/disassembly. *Cell Rep*, 37, 109917.
9. Fouquerel, E. and Sobol, R.W. (2014) ARTD1 (PARP1) activation and NAD(+) in DNA repair and cell death. *DNA Repair (Amst)*, 23, 27-32.
10. Al-Rahhalleh, R.Q. and Sobol, R.W. (2024) Poly(ADP-ribosyl)ation dynamics, signaling, and analysis. *Environ Mol Mutagen*, 65, 315-337.
11. Lord, C.J. and Ashworth, A. (2017) PARP inhibitors: synthetic lethality in the clinic. *Science*, 355, 1152-1158.

12. Li, J., et al. (2022) Overcoming temozolomide resistance via enhanced NAD+ bioavailability and inhibition of poly(ADP-ribose) glycohydrolase. *Cancers (Basel)*, 14, 103845.
13. Li, J. et al. (2021). NAD+ bioavailability mediates PARG inhibition–induced replication arrest, intra-S-phase checkpoint activation, and apoptosis. *NAR Cancer*, 3, zcab044.
14. Acharya, G. et al. (2024) CHK1 inhibitor–induced PARylation by targeting PARG causes replication stress and overcomes chemoresistance in ovarian cancer. *Cell Death Discov*, 10, 1-13.
15. Ravindranathan, R. et al. (2024). PARG inhibitor sensitivity correlates with accumulation of single-stranded DNA gaps in ovarian cancer models: *Proc Natl Acad Sci U S A*, 121, e2413954121.
16. Garcia-Diaz, M., et al. (2003). DNA polymerase λ, a novel DNA repair enzyme in human cells. *Mol Cell,* 11, 79–89.
17. Braithwaite, E.K., et al. (2005). DNA polymerase λ mediates a back-up base excision repair activity in extracts of mouse embryonic fibroblasts. *Mol Cell,* 17, 89–100.
18. Saville, K.M. et al. (2024) Oncometabolite 2-hydroxyglutarate suppresses basal protein levels of DNA polymerase beta that enhances alkylating agent and PARG inhibition induced cytotoxicity. *DNA Repair (Amst),* 140, 103700.
19. Khan, M.M. et al. (2025) DNA polymerase beta expression in head & neck cancer modulates the poly(ADP-ribose)-mediated replication checkpoint. *DNA Repair (Amst),* 150, 103853.

20. Ibrahim, M. et al. (2025) Replication-associated base excision repair/single-strand break repair regulates PARG inhibitor response via the PRMT1/PRMT5/ATR axis. *NAR Cancer*, 7, zcaf057.
21. Leonard, S.M. et al. (2026) Synergistic cellular toxicity from inhibition of poly(ADP-ribose) glycohydrolase (PARG) and ubiquitin-specific protease 1 (USP1). *Toxics*, 14, 162.
22. Hanzlikova, H. & Caldecott, K.W. (2019) Perspectives on PARPs and PARP inhibitors in DNA repair. *Nat Rev Mol Cell Biol*, 20, 405–421.
23. Lord, C.J. & Ashworth, A. (2012) The DNA damage response and cancer therapy. *Nature*, 481, 287–294.
24. Caldecott, K.W. (2022) DNA single-strand break repair and human genetic disease. *Trends Cell Biol*, 32, 733–745.

Figure Legends

Figure 1. siRNA-mediated knockdown of XRCC1 and POLB validated by immunoblot.

(A–C) Immunoblot of XRCC1 in whole cell lysates from cells transfected with non-targeting control siRNA (siNON) or XRCC1-targeting siRNA (siXRCC1). Panels A-C specify three independent biological replicates.

(D–F) Immunoblot of POLB in whole cell lysates from cells transfected with siNON or POLB-targeting siRNA (siPOLB). Panels D-F specify three independent biological replicates.

For all panels, histone H3 (H3) was employed as a loading control, and molecular weight markers are presented.

Figure 2. siRNA-mediated knockdown of LIG3 and APTX validated by immunoblot.

(A-C) Immunoblot analysis of LIG3 in whole-cell lysates following transfection with either non-targeting control siRNA (siNON) or LIG3-targeting siRNA (siLIG3). Panels A-C specify three independent biological replicates.

(D–F) Immunoblot analysis of APTX in whole-cell lysates from cells transfected with siNON or siAPTX. Panels D–F represent three independent biological replicates.

For all panels, histone H3 (H3) was employed as a loading control, and molecular weight markers are shown.

Figure 3. Knockdown of XRCC1 and POLB modulates cellular response to PARG inhibitor treatment.

(A-C) Cell viability (%) in response to increasing concentrations of PARG inhibitor (PARGi; 0–5 μM) in cells transfected with non-targeting control siRNA (siNON) or XRCC1-targeting siRNA (siXRCC1). Panels A-C specify three independent biological replicates.

(D-F) Cell viability (%) in response to PARGi (0–5 μM) in cells transfected with siNON or POLB-targeting siRNA (siPOLB). Panels D–F specify three independent biological replicates.

Cell viability was normalized to untreated controls. For all panels, cell viability was evaluated after 120 hours of exposure to the indicated concentrations of PARG inhibitor.

Figure 4. Knockdown of LIG3 and APTX differentially alters sensitivity to PARG inhibitor treatment.

(A–C) Cell viability (%) in response to growing concentrations of PARGi (0–5 μM) in cells transfected with siNON or LIG3-targeting siRNA (siLIG3). Panels A–C represent three independent biological replicates.

(D–F) Cell viability (%) in response to PARGi (0–5 μM) in cells transfected with siNON or APTX-targeting siRNA (siAPTX). Panels D–F specify three independent biological replicates.

Cell viability was normalized to untreated controls. For all panels, cell viability was evaluated after 120 hours of exposure to the indicated concentrations of PARG inhibitor.

Figure 1

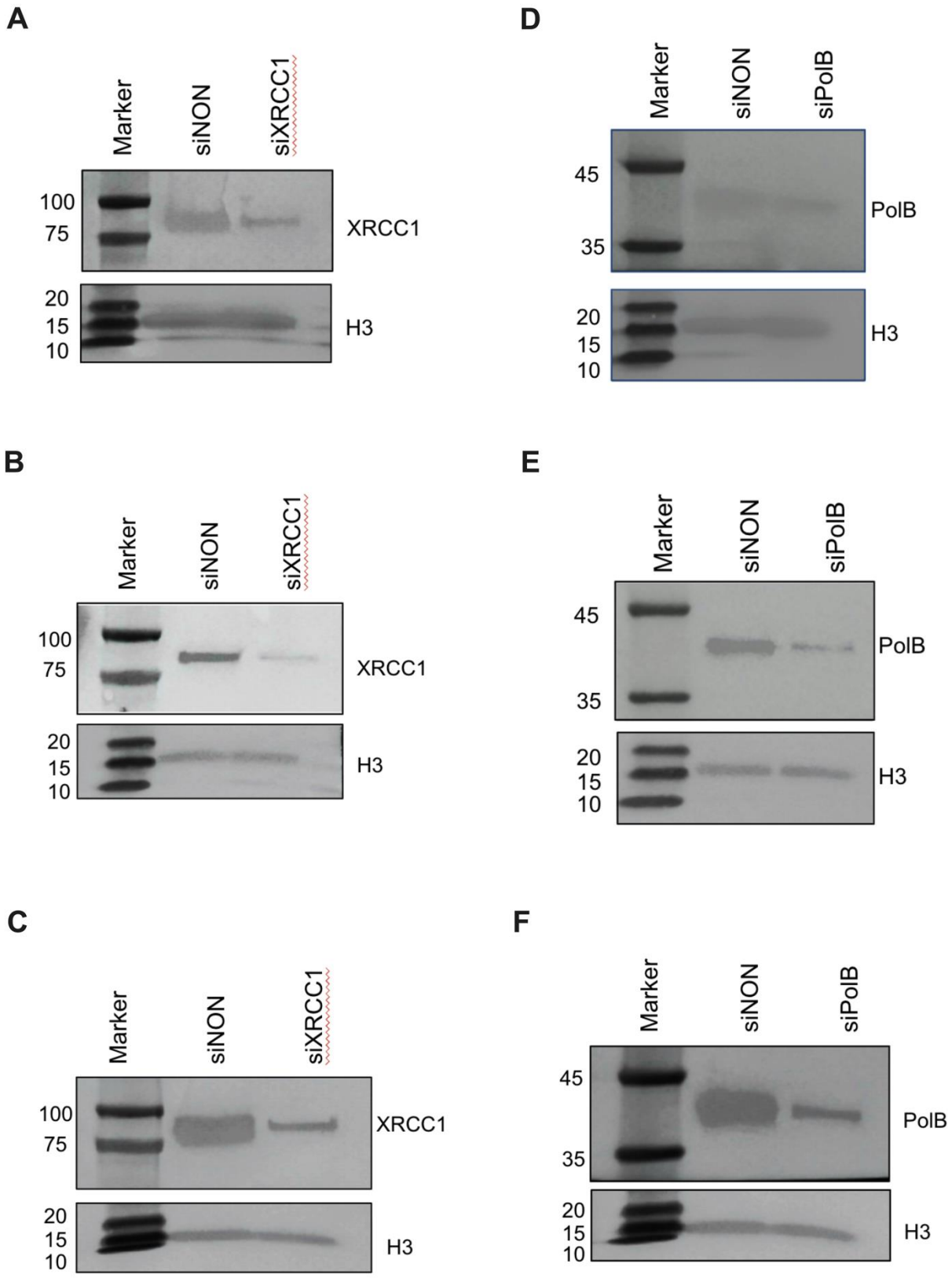

Figure 2

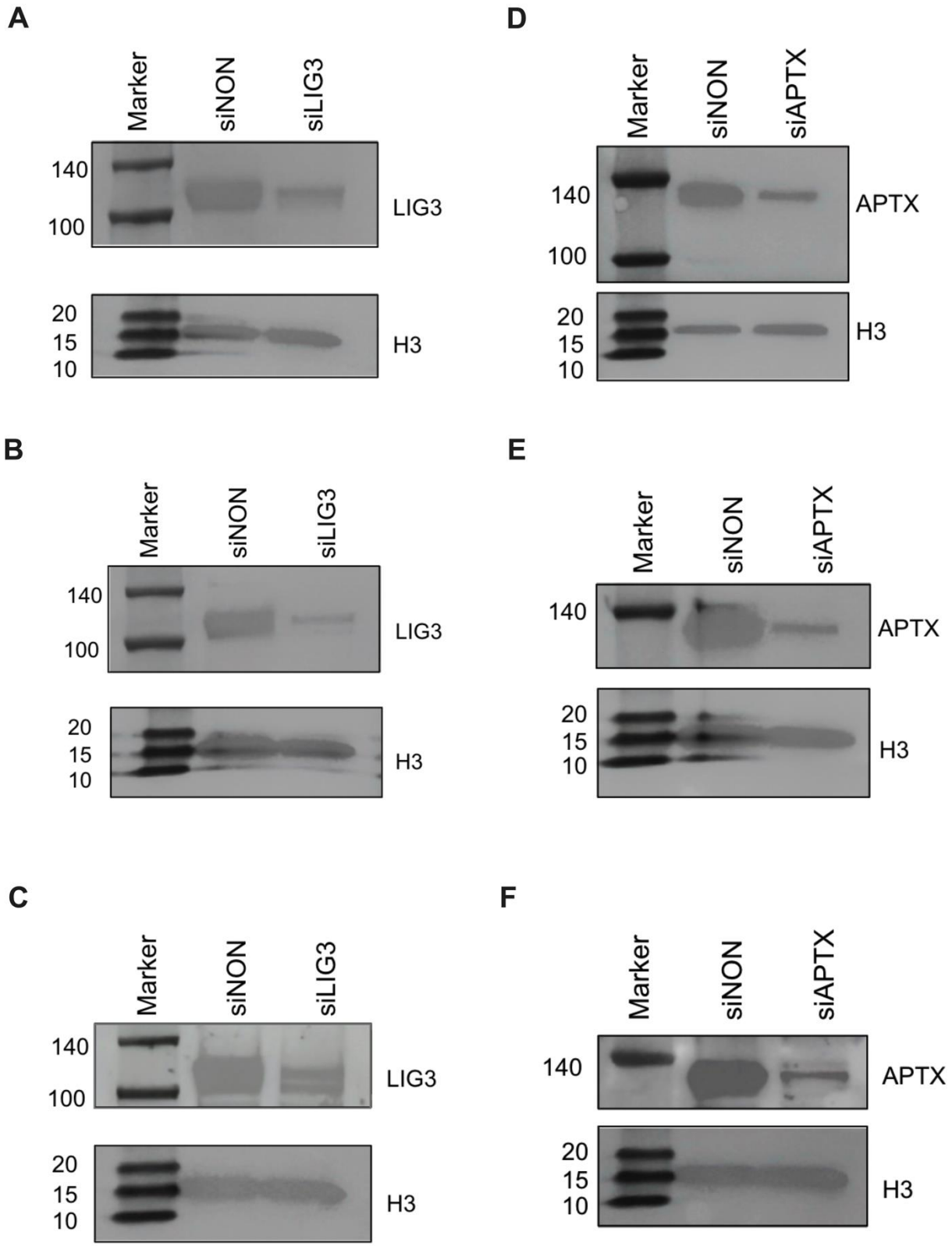

Figure 3

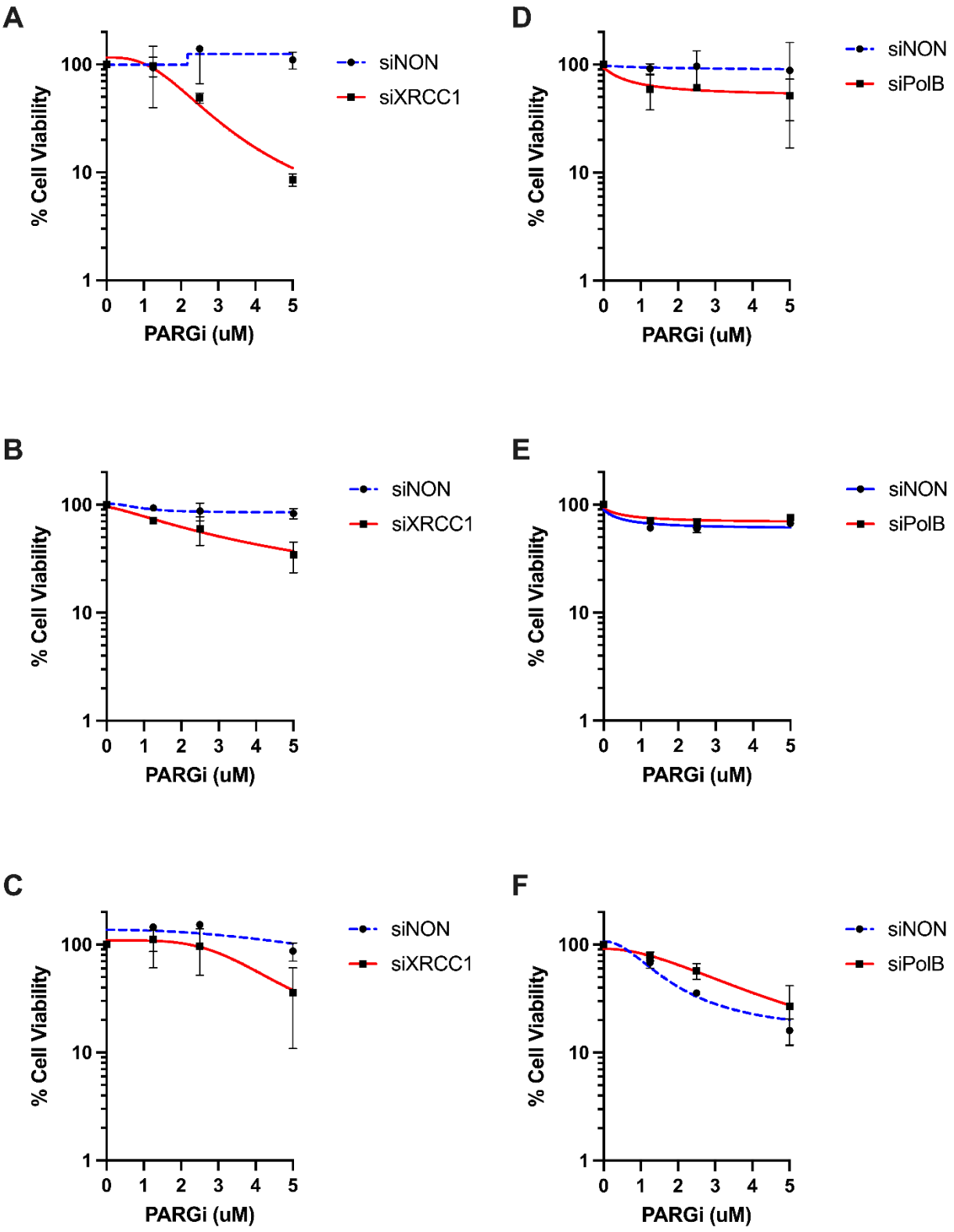

Figure 4

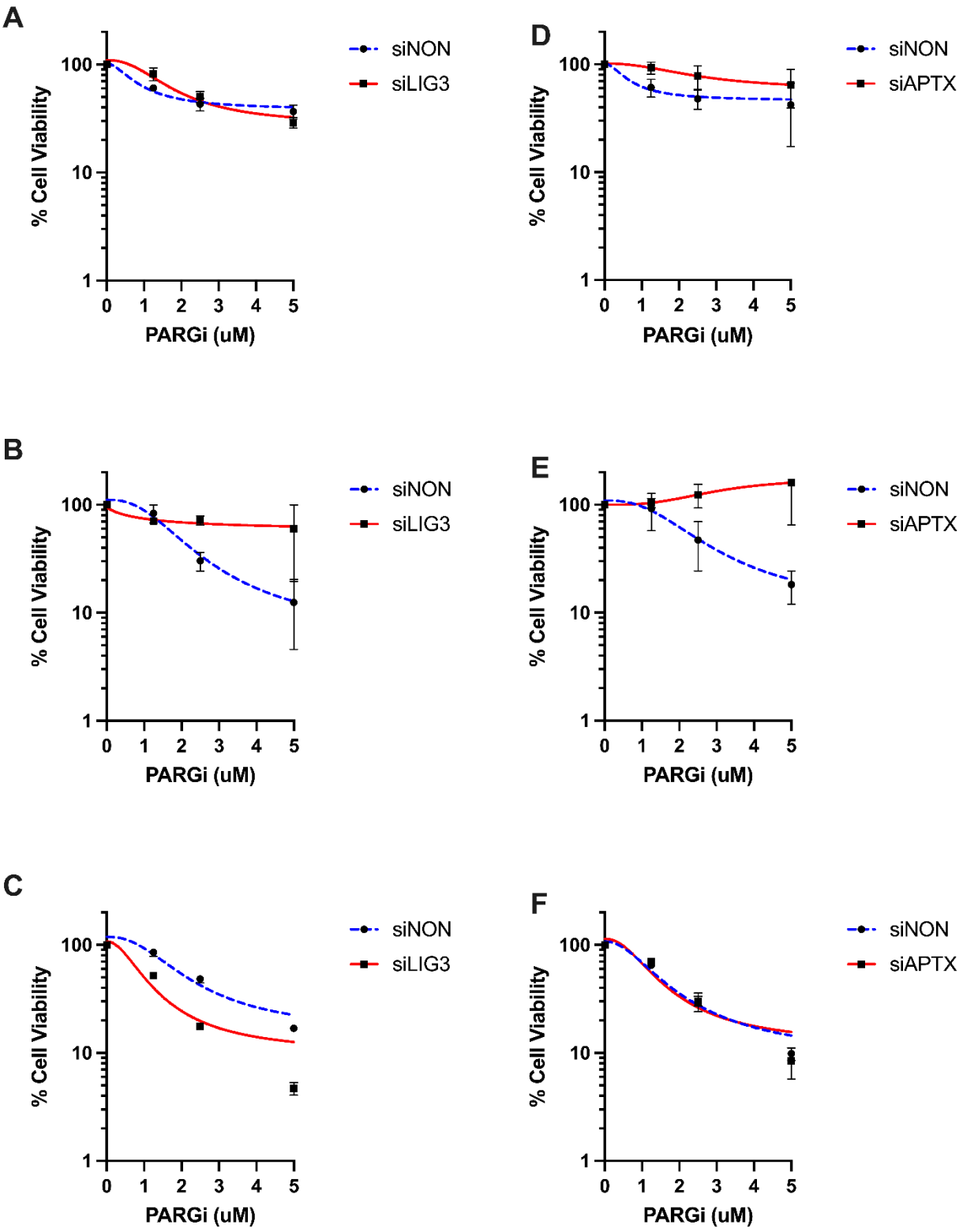

Table S1: Reagent List	**SOURCE**	**IDENTIFIER**
Antibodies (Use; Dilution)		
Histone H3 (D1H2) XP® Rabbit mAb (Immunoblot; 1:5000)	Cell Signaling Technology	Cat# 4499
Anti-XRCC1 antibody [EPR4389(2)] (Immunoblot; 1:1000)	Abcam	Cat# ab134056
Anti-DNA Polymerase beta antibody (Immunoblot; 1:1000)	Abcam	Cat# ab26343
Anti-DNA Polymerase beta antibody [EPR12722(B)] (Immunoblot; 1:1000)	Abcam	Cat# ab175197
Anti-DNA Ligase III/LIG3 antibody (AB223739) (Immunoblot; 1:500)	Abcam	Cat# ab223739
Anti-Aprataxin antibody [EPR8751] (Immunoblot; 1:1000)	Abcam	Cat# ab192598
Goat Anti-Rabbit IgG (H + L)-HRP Conjugate (Immunoblot; 1:2000)	Bio-Rad	Cat# 170-6515
Chemicals and reagent kits		
RPMI 1640,1X with L-glutamine	Corning	Cat# 10-040-CV
Heat-Inactivated Fetal bovine serum	Atlanta Biologics	Cat# S11150
L-glutamine	Gibco	Cat# 25030-081
0.25% Trypsin-EDTA (1x)	Gibco	Cat# 25200-056
DPBS, 1X	Corning	Cat# 21-031-CV

Penicillin/streptomycin	Thermo Fisher Scientific	Cat# 15140-122
DMSO (dimethyl sulfoxide)	Thermo Fisher Scientific	Cat# 3176
4X Laemmli Sample Buffer	Bio-Rad	Cat# 1610747
2-Mercaptoethanol	Aldrich	Cat# SHBH7147
20x MOPS buffer	Invitrogen	Cat# NP0001-02
Trans-Blot Turbo Mini-size Transfer Stacks	Bio-Rad	Cat# 1704270
Blotting-Grade Blocker	Bio-Rad	Cat# 1706404
Transblot Turbo Mini-size Nitrocellulose Membrane	Bio-Rad	Cat# 1704270
Trans-Blot Turbo 5x transfer buffer	Bio-Rad	Cat# 10026938
ExcelBand™ Enhanced 3-color High Range Protein Marker (9-245 kDa)	Smobio	Cat# PM2610
Nupage 4-12% Bis-Tris gel	Invitrogen	Cat# NP0323BOX
PARG inhibitor (PDD00017272)	Tocris	Cat# 7006
Lipofectamine™ RNAiMAX Transfection Reagent	Thermo Fisher Scientific	Cat# 13778075
Opti-MEM™ I Reduced Serum Medium	Thermo Fisher Scientific	Cat# 31985062
Ethanol	Decon Labs	Cat# 3916EA
Hoechst 33342	Thermo Fisher Scientific	Cat# 62249
Propidium Iodide	Sigma-Aldrich	Cat# P4170

siGENOME Non-Targeting siRNA Pool #1	Horizon	Cat# D-001206-13-05
siGENOME Human POLB (5423) siRNA	Horizon	Cat# M-005164-01-0005
siGENOME Human XRCC1 (7515) siRNA	Horizon	Cat# M-009394-01-0005
siGENOME Human APTX (54840) siRNA	Horizon	Cat# M-013368-02-0005
siGENOME Human LIG3 (3980) siRNA	Horizon	Cat# M-009227-02-0005
Cell lines		
ES-2 (Human ovarian clear cell carcinoma)	ATCC	Cat# CRL-1978
Software and Algorithms		
GraphPad Prism	GraphPad	Version 10.2.2 (Mac OS X)